

# Kondo Effect in Fermi Systems with a Gap: A Renormalization Group Study

Kan Chen<sup>(1)</sup> and C. Jayaprakash<sup>(2)</sup>

<sup>(1)</sup>*Department of Computational Science, National University of Singapore, Singapore 119260  
and*

<sup>(2)</sup>*Department of Physics, The Ohio State University, Columbus, OH 43210, U.S.A.  
(February 1, 2008)*

We present the results of a Wilson Renormalization Group study of the single-impurity Kondo and Anderson models in a system with a gap in the conduction electron spectrum. The behavior of the impurity susceptibility and the zero-frequency response function,  $T \ll S_z; S_z \gg$  are discussed in the cases with and without particle-hole symmetry. In addition, for the asymmetric Anderson model the correlation functions,  $\langle \vec{S} \cdot \vec{\sigma}(0) \rangle$ ,  $\langle n_d \rangle$ , and  $\langle n_d(2 - n_d) \rangle$  are computed.

PACS numbers: 75.20.Hr, 75.30.Mb, 75.20.Ck

## I. INTRODUCTION

The properties of a magnetic impurity in a semiconductor or an insulator are of interest for a variety of reasons. In a normal fermi system a spin- $\frac{1}{2}$  impurity yields logarithmic temperature dependences in the impurity susceptibility and the resistivity at high temperatures; at low temperatures the magnetic moment is quenched<sup>1,2</sup>. The existence of a sharp fermi surface and the concomitant occurrence of (low-energy) particle-hole pairs play an important role in understanding the behavior of the model. Thus it is interesting from a theoretical point of view to understand whether the Kondo effect persists and under what conditions quenching occurs in a system with a gap and determine the behavior quantitatively. We also note that the Anderson impurity has been studied in the context of the logarithmic temperature dependence of the conductivity of trans-polyacetylene<sup>4</sup>; the system was modeled by a continuum Hamiltonian that exhibits a gap due to Peierls distortion. The impurity model was investigated using a Hartree-Fock closure of the equation of motion. In addition, a variety of Kondo and valence fluctuating insulators (modeled theoretically by a Kondo or Anderson lattice) such as  $SmB_6$  and  $Ce_3Bi_4Pt_3$  among others provide another motivation for studying the single impurity problem in a system with a gap.

In this paper we present the results of our study of the Kondo and Anderson impurities in a system with a gap. We apply Wilson's (numerical) Renormalization Group (RG) technique using a variant of a numerical tridiagonalization method devised by us earlier<sup>6</sup> and provide results for both the susceptibility and zero-frequency response functions. We also discuss a simple effective Hamiltonian that allows us to understand the physics underlying our results.

We begin with a summary of previous work on the problem; in the next section we provide a brief sketch of the technique that is described in detail in the literature<sup>3</sup>. We then present the results of our numerical simulations and in the final section we discuss the effective Hamiltonian description of our results.

We begin with a brief overview of previous work. The first calculations were done by Ogura and Saso<sup>9-11</sup> and Takegahara *et al.*<sup>12,13</sup>. Ogura and Saso used a  $1/N$  expansion of the degenerate Anderson model and found to leading order a transition between the triplet and singlet ground states when the gap  $E_g$  equals twice the Kondo temperature  $T_K$ . In their Quantum Monte Carlo (QMC) simulations they found indications of a similar transition even for the symmetric Anderson model<sup>9</sup>; for the asymmetric model they obtained a transition between the different ground states at approximately  $E_g \approx 3T_K$ . We note that their QMC computations were limited to temperatures above  $T_K/10$ .

Takegahara, Shimizu, and Sakai<sup>12,13</sup> used both Quantum Monte Carlo simulations and the numerical Renormalization group method of Wilson. They considered the symmetric Anderson model and found that at low temperatures the susceptibility follows a Curie law resulting from an unquenched magnetic moment. They observed the crucial difference between symmetric and asymmetric Anderson models cases; when particle-hole symmetry is obeyed the moment remains unquenched for all non-zero values of the gap while there is a transition in the asymmetric case. They also used the Wilson numerical Renormalization group to follow the spectrum of the low-energy states but not the susceptibility. It is difficult to use their version of the numerical RG formulation to calculate low temperature (much less than the band gap) properties of the model.

Yu and Guerrero<sup>14</sup> studied an Anderson impurity in a semiconducting host using the density matrix renormalization technique. Their calculation which is restricted to  $T = 0$  considered electron spin-impurity spin correlation functions and found no *qualitative difference* between the symmetric and asymmetric cases. We will comment on this point later. The importance of the particle-hole symmetry breaking has been emphasized recently<sup>15</sup> in the context of the Kondo problem with a pseudogap. In this work the impurity susceptibility for the case of a Kondo system with a gap was also calculated using the Wilson renormalization group method: in the particle-hole symmetric case the impurity

retains its moment in the ground state for all  $J$ ; in the presence of potential scattering the moment is completely quenched provided that  $\Delta \ll T_K$ . These results are in agreement with those of Takegahara *et al*<sup>12,13</sup>.

We have made a comprehensive study of the Kondo and Anderson models in gapped systems with and without particle-hole symmetry breaking using the numerical RG method. Our RG formulation is based on the numerical tridiagonalization technique developed by us<sup>6</sup>, which allows us to calculate various quantities in the entire temperature range. We report results for a zero-frequency response function, correlation functions and the susceptibility: we emphasize the differences in their behaviors in the various regimes and clarify which of these are good probes of the nature of the low-temperature fixed point behavior.

## II. WILSON'S RG FORMULATION

We consider the Kondo and Anderson models with a conduction electron Hamiltonian with the density of states  $\rho(\epsilon)$ ; as a function of the energy  $\epsilon$ ,  $\rho$  is a constant for  $D_0 > |\epsilon| > \Delta_0$ , where the band edges lie at  $\pm D_0$  from the Fermi level which is chosen to be in the middle of the gap. The width of the gap is thus  $2\Delta_0$ . The impurity part of the Hamiltonian for the spin- $\frac{1}{2}$  Kondo problem with the impurity spin denoted by  $\vec{S}$  is given in standard notation by

$$H_K = -J \sum_{\mu, \nu} \int_{-D_0}^{D_0} d\epsilon \sqrt{\rho(\epsilon)} \int_{-D_0}^{D_0} d\epsilon' \sqrt{\rho(\epsilon')} \vec{S} \cdot c_{\epsilon, \mu}^+ \frac{1}{2} \vec{\sigma}_{\mu\nu} c_{\epsilon', \nu} + K \sum_{\mu} \int_{-D_0}^{D_0} d\epsilon \sqrt{\rho(\epsilon)} \int_{-D_0}^{D_0} d\epsilon' \sqrt{\rho(\epsilon')} c_{\epsilon, \mu}^+ c_{\epsilon', \mu} \quad ; \quad (1)$$

for the Anderson model we have

$$H_A = (\epsilon_d + \frac{U}{2}) \sum_{\mu} c_{d\mu}^+ c_{d\mu} + \frac{U}{2} \left( \sum_{\mu} c_{d\mu}^+ c_{d\mu} - 1 \right)^2 + \sum_{\mu} \int_{-D_0}^{D_0} d\epsilon \sqrt{\rho(\epsilon)} [V c_{\epsilon, \mu}^+ c_{d\mu} + V^* c_{d\mu}^+ c_{\epsilon, \mu}] \quad , \quad (2)$$

where  $c_{d\mu}^+$  creates an electron with spin  $\mu$  at the impurity placed at the origin. The choice  $K = 0$  in the Kondo problem and  $\epsilon_d + \frac{U}{2} = 0$  in the Anderson model correspond to particle-hole symmetry.

Following Wilson we perform a *logarithmic* discretization of the energy variable; we rescale the energy by  $D_0$  so that  $\epsilon \in [-1, 1]$ , introduce a scale factor  $\Lambda (> 1)$ , and define the  $n$ th interval for positive  $\epsilon$  to lie between  $\Lambda^{-n-1}$  and  $\Lambda^{-n}$ . The band gap is chosen to be

$$\Delta = \Lambda^{-M_0} \quad .$$

Next we replace the continuous set of energy levels in the  $n$ th interval  $[\Lambda^{-n-1}, \Lambda^{-n}]$  and  $[-\Lambda^{-n}, -\Lambda^{-n-1}]$  by single levels at  $(\Lambda^{-n-1} + \Lambda^{-n})/2$  and  $-(\Lambda^{-n-1} + \Lambda^{-n})/2$  respectively, and introduce  $a_{n\mu}^+, b_{n\mu}^+$ , the conduction electron creation operators for the states with the corresponding energies  $(\Lambda^{-n-1} + \Lambda^{-n})/2$  and  $-(\Lambda^{-n-1} + \Lambda^{-n})/2$ . After this discretization, the Anderson Hamiltonian can be rewritten in the following form<sup>3</sup> (Here we only consider the Anderson Hamiltonian; similar RG formulation can be written down for the Kondo Hamiltonian)

$$H_A = \frac{1 + \Lambda^{-1}}{2} \sum_{m=0}^{M_0-1} \Lambda^{-m} (a_{m\mu}^+ a_{m\mu} - b_{m\mu}^+ b_{m\mu}) + (\epsilon_d + \frac{1}{2}U) c_{d\mu}^+ c_{d\mu} + \left[ \frac{2\Gamma}{\pi} \right]^{\frac{1}{2}} (f_{0\mu}^+ c_{d\mu} + c_{d\mu}^+ f_{0\mu}) + \frac{U}{2} (c_{d\mu}^+ c_{d\mu} - 1)^2 \quad , \quad (3)$$

where

$$f_{0\mu} = \sqrt{\frac{1 - \Lambda^{-1}}{2(1 - \Delta)}} \sum_{m=0}^{M_0-1} \Lambda^{-m/2} (a_{m\mu} + b_{m\mu}) \quad .$$

The initial values of the couplings  $\Gamma$  ( $\equiv 0.5\pi V^2$ ),  $\epsilon_d$ , and  $U$ , are now in units of  $D_0$  (taken to be one); the gap in the density of states is between  $\Delta$  and  $-\Delta$ .

We use the (numerical) tridiagonalization scheme devised by us earlier<sup>6</sup> to transform the Hamiltonian to the following tridiagonalized form:

$$H_A = \frac{1 + \Lambda^{-1}}{2} \sum_{n=0}^{N_0-1} [\xi_n (f_{n\mu}^+ f_{n+1\mu} + h.c.)] + (\epsilon_d + \frac{1}{2}U) c_{d\mu}^+ c_{d\mu} + \left[ \frac{2\Gamma}{\pi} \right]^{\frac{1}{2}} (f_{0\mu}^+ c_{d\mu} + c_{d\mu}^+ f_{0\mu}) + \frac{U}{2} (c_{d\mu}^+ c_{d\mu} - 1)^2, \quad (4)$$

where  $N_0 = 2M_0 - 1$ .

In order to carry out the RG calculation, we need to rescale the Hamiltonian at each iteration step. The rescaling is done by defining  $H_N$  as follows:

$$H_N = \frac{1}{\xi_{N-1}} \left[ \sum_{n=0}^{N-1} [\xi_n (f_{n\mu}^+ f_{n+1\mu} + h.c.)] \right] + \frac{1}{\xi_{N-1}} \left[ (\tilde{\epsilon}_d + \tilde{U}) c_{d\mu}^+ c_{d\mu} + \tilde{\Gamma}^{\frac{1}{2}} (f_{0\mu}^+ c_{d\mu} + c_{d\mu}^+ f_{0\mu}) + \tilde{U} (c_{d\mu}^+ c_{d\mu} - 1)^2 \right], \quad (5)$$

where  $\tilde{\epsilon} = \frac{2}{1+\Lambda^{-1}}\epsilon_d$ ,  $\tilde{U} = \frac{U}{1+\Lambda^{-1}}$ ,  $\tilde{\Gamma} = [\frac{2}{1+\Lambda^{-1}}]^2 \frac{2\Gamma}{\pi}$ , and the rescaling factor is  $S_N = \frac{2}{(1+\Lambda^{-1})\xi_{N-1}}$ .

The recursion relation can be written in the following compact form:

$$H_{N+1} = \frac{\xi_{N-1}}{\xi_N} H_N + (f_{N\mu}^+ f_{N+1\mu} + h.c.).$$

This recursion relation enables one to set up an iterative diagonalization scheme to calculate the energy levels of  $H_N$  and thus to determine thermodynamic properties; the recursion is implemented numerically and is stopped at  $N = N_0$  corresponding to the edge of the gap below which there are no conduction electron states. Recall that as we increase  $N$ , the system effectively evolves from high temperatures to low temperatures. At a given  $N$ , the thermodynamic quantities are calculated for  $T_N = 1/(\bar{\beta}S_N)$  for a selected values of  $\bar{\beta}$ . By studying the evolution of the many-body energy level structures we also obtain information near the fixed points of the Hamiltonian.

For  $N < N_0$ , the thermodynamic quantities are calculated for  $T_N = 1/(\bar{\beta}S_N)$  for a selected value of  $\bar{\beta}$ ; the accuracy of the numerical evaluations is enhanced by performing a second-order perturbation calculation by writing the Hamiltonian as

$$H_A = (H_N + H_I + H_B)/S_N,$$

where

$$H_I = \frac{\xi_N}{\xi_{N-1}} (f_{N\mu}^+ f_{N+1\mu} + h.c.),$$

and

$$H_B = \frac{1}{\xi_{N-1}} \left\{ \sum_{n=N+1}^{N_0-1} [\xi_n (f_{n\mu}^+ f_{n+1\mu} + h.c.)] \right\}.$$

For  $N = N_0$ , the thermodynamic quantities are calculated for a sequence of temperatures  $\{T_l\}$ . Since  $H_{N_0}$  is the full Hamiltonian (hence, no second order perturbation is needed), we can calculate the quantities at temperatures much lower than typical energy scale at  $N = N_0$ , which is the bandgap  $\Delta$ . We choose  $T_l$  to be a sequence of values from 0.175 of the maximum energy kept in the many body states of  $H_{N_0}$  to 0.000175 of the maximum energy. Thus the thermodynamic quantities at low temperatures are calculated with the “effective Hamiltonian”  $H_{N_0}$ .

### III. RESULTS

We present the results obtained from our numerical calculations for the two models.

## A. Kondo Model

Our calculations were performed using a scale factor of  $\Lambda = 2$  and a band gap energy  $\Delta = 1.22 \times 10^{-4}$  corresponding to  $M_0 = 13$ . The first and obvious quantity to consider is the impurity susceptibility,  $\chi$ , which we emphasize is defined as the total susceptibility of the system minus the susceptibility of the pure system. In the Kondo problem in the absence of potential scattering  $T\chi$  approaches the value  $1/4$  as  $T \rightarrow 0$  for *any* finite bandgap. The ground state is a magnetic doublet, its quantum numbers are ( $Q = 0$ ,  $S = 1/2$ ). This is in agreement with the results of Takegahara et al<sup>13</sup> for the symmetric Anderson model. The susceptibility curves are displayed in Fig. 1(a). Note that some data obtained at intermediate points have been suppressed for clarity in this figure as well as in other figures we are going to present in this paper. The calculation is done for initial values of the coupling given by  $J_0 = -0.1, -0.2, -0.3, -0.4, -1.0$ . Note that for large values of  $|J|$  the universal shape of  $T\chi$  of the ordinary Kondo problem is evident at high temperatures but below temperatures of the order of the gap  $T\chi$  increases sharply.

The effect of particle-hole symmetry breaking introduced by potential scattering is very important as has been noted before<sup>15,12</sup>. The results for  $T\chi$  are displayed in Fig. 1(b). For  $K_0 = 0.1$  and  $J_0 = -0.2$  ( $T_K \approx 7.4 \times 10^{-6} \ll \Delta$ ),  $T\chi$  again goes to  $1/4$  as  $T$  goes to zero. For stronger Kondo coupling,  $J = -0.4$  ( $T_K \approx 2.1 \times 10^{-3} \gg \Delta$ ), the impurity spin is quenched and  $T\chi \rightarrow 0$ . There is a discontinuous (“first-order”) transition due to a crossing of energy levels. Crudely speaking, in the generic case without particle-hole symmetry, the transition occurs when the energy gained by forming the singlet which is of the order of  $T_K$  is larger than the energy required to create a particle-hole excitation across the gap.

We have also calculated the zero-frequency response function  $T \langle\langle S_z; S_z \rangle\rangle$ . The techniques for performing such calculations have been explained in an earlier paper for the ordinary Kondo problem<sup>7</sup>. We used  $\Lambda = 3.0$  in the calculation of the response function. Note that for the ordinary Kondo problem  $\langle\langle S_z; S_z \rangle\rangle$  is essentially the same as the impurity susceptibility  $\chi$  for small values of the initial coupling<sup>7</sup>. However, for the density of states with a gap,  $\langle\langle S_z; S_z \rangle\rangle$  and  $\chi$  behave quite differently at low temperatures (when  $T < \Delta$ ). In the absence of potential scattering, in contrast to  $T\chi$  which approaches a fixed value of  $1/4$  as  $T \rightarrow 0$ ,  $T \langle\langle S_z; S_z \rangle\rangle$  approaches a value  $C_0$  which depends on the bandgap; this persists also when the moment is not quenched in the presence of potential scattering. The results for  $C_0$  are listed in Table I. For  $K = 0$  our results are consistent with the value  $C_0$  being proportional to  $\Delta^2$  for  $\Delta \ll T_K$ . We will derive this result from our effective Hamiltonian description in the next section. This result agrees with the claim made by Takegahara et al. for the susceptibility<sup>12</sup>; we note that they appear to have identified  $\langle\langle S_z; S_z \rangle\rangle$  with the impurity susceptibility. In the presence of potential scattering when  $\Delta$  is increased for fixed  $T_K$  the ground state changes abruptly from a singlet [ $(Q = -1, S = 0)$ ] to a doublet. The value of  $T\chi$  jumps from 0 to  $1/4$  and correspondingly the value of  $C_0$  also jumps discontinuously.

## B. Anderson Model

The calculations for the Anderson model were performed with the parameter  $\Lambda = 3$ . A range of values was used for the band gap  $\Delta = \Lambda^{-M_0}$ : the value of  $M_0$  was varied between 3 and 19.

For the symmetric Anderson Model, with  $U = 0.1$ ,  $\epsilon_d = -\frac{U}{2} = -0.05$ , and  $\Gamma = 0.006$ ,  $T\chi$  reaches the value of  $1/4$  as zero temperature is approached irrespective of the value of the bandgap  $\Delta$ , signaling a doublet ground state and an unquenched impurity moment. If  $\Delta \ll T_K \approx 5.12 \times 10^{-6}$ ,  $T\chi$  first decreases toward zero along the universal Kondo curve; however, when  $T < \Delta$ , it rises to  $1/4$  as  $T$  goes to zero. If  $\Delta$  is comparable or larger than  $T_K$ , on the other hand,  $T\chi$  gradually increases to  $1/4$ . Our results for  $T\chi$  are displayed in Fig. 2(a).

The case of the the asymmetric Anderson Model was studied using the parameter values  $U = 0.1$ ,  $\epsilon_d = -0.0001$ , and  $\Gamma = 0.00015$ , and the results are displayed in Fig. 2(b). When  $\Delta = 0$ , the system goes successively through the free-orbital regime, the mixed valence regime, the local moment regime, and the frozen moment regime<sup>3</sup>. When  $\Delta \neq 0$ , for  $T > \Delta$ , the  $T\chi$  curve initially follows the curve for  $\Delta = 0$  as the temperature is lowered. When  $T$  drops below  $\Delta$ ,  $T\chi$  curves starts to rise. For  $\Delta > T_K$ , the curve continues to rise to  $1/4$  as  $T$  goes to zero. On the other hand, when  $\Delta < T_K$ , the curve stops rising, turns over and tends to zero as  $T \rightarrow 0$ . This behavior is clearly similar to that of the  $K \neq 0$  case of the Kondo model.

Fig. 3 shows the general temperature dependences of the zero-frequency response function  $T \langle\langle S_z; S_z \rangle\rangle$  for the asymmetric case. There is no qualitative difference in the behavior of the response function  $T \langle\langle S_z; S_z \rangle\rangle$  between the Kondo and Anderson models. In the symmetric case where the ground state is characterized by ( $Q = 0, S = 1/2$ ), we again found that the zero-temperature value  $C_0$  is proportional to  $\Delta^2$  when  $\Delta$  decreases. Also for the asymmetric case  $C_0$  jumps discontinuously as the ground state changes from a singlet to a doublet as  $\Delta$  is increased.

In addition, we have also computed the following correlation functions:  $\langle \vec{S} \cdot \vec{\sigma}(0) \rangle$ ,  $\langle n_d \rangle$ , and  $\langle n_d(2 - n_d) \rangle$ . Representative figures are shown in Fig. 4(a), and Fig. 4(b). Here the main point to be emphasized is that once there

are no charge fluctuations (for example, when the system approaches the local moment regime, or when  $T < \Delta$ ) the correlation functions do not change and approach constant values. In particular, when the local moment regime is reached ( $\Delta$  is less than the temperature for the local moment formation), the correlation functions tend to the same constants as  $T \rightarrow 0$  independent of the band gap. While the mixed valence regime is still reflected in the temperature dependence of the correlation functions, the Kondo effect does not show up in the correlation functions. This point is not very well appreciated. One simply *cannot* investigate the Kondo effect using *local* correlation functions, such as the impurity spin-conduction electron spin-density at the origin, since they do not contain information about the system on the energy scale of  $T_K$  or equivalently the length scale of  $\hbar v_e/T_K$  where  $v_e$  is the characteristic velocity of the electrons. We believe that this is the reason why in the work of Yu and Guerrero<sup>14</sup> no difference was found between the symmetric and asymmetric Anderson models in the correlation functions at short length scales.

Finally, we present our results for the mixed-valent regime. We considered the asymmetric Anderson Model, with  $U = 0.1$ ,  $\epsilon_d = -0.025$ , and  $\Gamma = 0.01$ . When  $\Delta = 0$ , the system goes from the free-orbital regime through the mixed valence regime directly to the frozen moment regime, without going through the local moment regime. The results for the susceptibility,  $\langle n_d \rangle$ , and  $T \ll S_z; S_z \gg$  are shown in Fig. 5(a)-(c). Again, depending on the value of the band gap,  $T\chi$  can go to zero or  $1/4$  (there is a sharp transition). For the cases that  $T\chi$  goes to zero,  $T \ll S_z; S_z \gg$  also goes to zero, and all correlation functions approach constants, which are independent of the band gap. But for the cases that  $T\chi$  goes to  $1/4$ , both  $T \ll S_z; S_z \gg$  and the correlation functions approach the values which are band-gap dependent.

#### IV. EFFECTIVE HAMILTONIAN DESCRIPTION

In this section we provide a simple interpretation of the low-temperature behavior of the models in the various regimes on the basis of a simple effective Hamiltonian. Let us consider first the Kondo Model with the gap in the conduction electron density of states between  $-\Delta$  to  $\Delta$ . The initial couplings are  $J_0$  and  $K_0$  in units of the bandwidth  $D_0$ , which is taken to be unity. In our RG calculation, the band gap is taken to be  $\Delta = \Lambda^{-M_0}$ , where  $M_0$  is an integer; this corresponds to the maximum  $N$  being  $N_0 = 2M_0 - 1$  — there are even number of conduction electron levels in the discretized system.

Imagine that we have successively integrated out the high energy degrees of freedom and arrived at the effective Hamiltonian at the energy scale  $\Delta \equiv \Lambda^{-(N_0+1)/2}$ ; as we pointed out earlier the iterative RG procedure cannot be carried beyond this energy scale corresponding to the maximum iteration number  $N_0$  since there are no conduction electron states left. The low temperature properties (i.e. for  $T \ll \Delta$ ) can be calculated with this effective Hamiltonian.

Let us consider the case when  $\Delta \gg T_K$ . The effective Hamiltonian is close to that of the  $J = 0$  fixed point and can be written, keeping the leading order terms, as

$$H_{eff} = -J\vec{S} \cdot \vec{\sigma}(0) + K f_\mu^+ f_\mu + \Delta(a_\mu^+ a_\mu - b_\mu^+ b_\mu) \quad .$$

Here  $\vec{\sigma}(0) = \frac{1}{2} f_\mu^+ \vec{\sigma}_{\mu\nu} f_\nu$  and  $f_\mu = \frac{1}{\sqrt{2}}(a_\mu + b_\mu)$ . In the above effective Hamiltonian we have only kept the lowest single electron/hole levels of the conduction electron Hamiltonian; these are represented by the creation operators  $a_\mu^+$  and  $b_\mu^+$  and we have neglected the irrelevant operators. Since  $f_0$  is proportional to  $\Lambda^{-N_0/4}$ , we have<sup>1</sup>

$$f_{0\mu} = \alpha_0 \Lambda^{-N_0/4} (a_\mu + b_\mu) + \dots$$

Thus the first two terms of  $H_{eff}$  are marginal, and  $J$  and  $K$  must scale as  $J = J_0 \Delta$  and  $K = K_0 \Delta$ . When  $|J_0| \ll 1$  and  $|K_0| \ll 1$ , the last term dominates, and the ground state is a doublet.

Next we consider the case  $\Delta \ll T_K$ . As we lower the energy scale to  $\Delta$ , the operator  $f_0$  or  $f$  is frozen, but  $f_1$  is proportional to  $\Lambda^{-N_0/4}$ :

$$f_{1\mu} = \hat{\alpha}_0 \Lambda^{-N_0/4} g_\mu + \dots$$

The operator  $g$  represents the single electron level at zero energy (the number of electron levels is odd, since  $f_0$  is frozen).

Now the effective Hamiltonian (at the energy scale  $\Delta$ ) can be written as

$$H_{eff} = -J\vec{S} \cdot \vec{\sigma}(0) + K f_\mu^+ f_\mu + w(f^+ g + h.c.) \quad . \quad (6)$$

The operators  $f$  and  $g$  arise when we express  $f_0$  and  $f_1$  in terms of the lowest single electron/hole levels of the conduction electron Hamiltonian. In the effective Hamiltonian given above  $J$  and  $K$  are renormalized coupling

constants; they increase in magnitude as the high-energy degrees of freedom are integrated out but they saturate at the value attained at an energy scale of  $T_K$  and are not further altered (since  $f$  is frozen); however, the coupling constant  $w$  will continue to scale as  $w \propto \Lambda^{-N_0/4}$  when  $N_0$  increases (or as  $\Delta$  decreases), we expect  $w \propto \sqrt{\Delta}$ . Since  $w$  should be of the order of  $T_K$  when  $\Delta = T_K$ , we can re-write  $w = \alpha T_K \sqrt{\Delta/T_K}$ . Note that in writing down the above Hamiltonian we have neglected all irrelevant terms, the inclusion of which will not change the results qualitatively.

We want to investigate the nature of the ground states of the above Hamiltonian for the cases  $K_0 = 0$  and  $K_0 \neq 0$ , by diagonalizing the Hamiltonian. This is mildly tedious but can be carried out in a straightforward fashion. The main results are as follows: The ground state is always a singlet (when  $K > 0$ , the ground state is in the subspace  $(Q = -1, S = 0)$  (for  $K < 0$ , it is in the subspace  $(1, 0)$ ). The first excited state is in the subspace  $(0, 1/2)$  and has a gap relative to the ground state proportional to  $\Delta$ . For  $K = 0$ , the ground state is in the subspace  $(0, 1/2)$ , which is a doublet with the energy gap to the first excited state proportional to  $\Delta^2$ . These results are in agreement with our numerical RG computations. For the benefit of the reader a derivation of these results is presented below.

### A. Diagonalizing the effective Hamiltonian

We diagonalize  $H_{eff}$  in Equation (6) in two steps. Diagonalizing the first two terms of the Hamiltonian  $H_{eff}$  in the subspace of the  $f$  states gives rise to four eigenstates given below:

- State A  $(-1, 1/2)$ :  $E = 0$
- State B  $(0, 0)$ :  $E = \frac{3}{4}J + K$
- State C  $(0, 1)$ :  $E = -\frac{1}{4}J + K$
- State D  $(1, 1/2)$ :  $E = 2K$

Here the numbers in the parentheses denote the charge and spin of the energy states.

Now we add the  $g$  states. The Hamiltonian can be written in the basis consisting of A, B, C, D and  $g$  states using a procedure similar to what was employed in the iteration scheme of Wilson's RG iteration (see for example, Eqn. (B2) in Appendix B of the paper by Krishna-murthy et al<sup>3</sup>). Let A1, A2, A3, A4 denote the basis states obtained by combining A with zero, one, and two  $g$  states, etc. The Hamiltonian matrix in each charge-spin subspace can be written down as

- State A1  $(2, 1/2)$ :  $H_{2,1/2} = 0$
- State A3+B1  $(-1, 0)$ :

$$H_{-1,0} = \begin{pmatrix} 0 & w \\ w & \frac{3}{4}J + K \end{pmatrix}$$

- State A2+C1  $(-1, 1)$ :

$$H_{-1,1} = \begin{pmatrix} 0 & w \\ w & -\frac{1}{4}J + K \end{pmatrix}$$

- State A4+B2+C3+D1  $(0, 1/2)$ :

$$H_{0,1/2} = \begin{pmatrix} 0 & \frac{w}{\sqrt{2}} & -\sqrt{\frac{3}{2}}w & 0 \\ \frac{w}{\sqrt{2}} & \frac{3}{4}J + K & 0 & \frac{w}{\sqrt{2}} \\ -\sqrt{\frac{3}{2}}w & 0 & -\frac{1}{4}J + K & -\sqrt{\frac{3}{2}}w \\ 0 & \frac{w}{\sqrt{2}} & -\sqrt{\frac{3}{2}}w & 2K \end{pmatrix}$$

- State C2  $(0, 3/2)$

$$H_{0,3/2} = -\frac{1}{4}J + K$$

- State B4+D3 (1, 0):

$$H_{1,0} = \begin{pmatrix} \frac{3}{4}J + K & -w \\ -w & 2K \end{pmatrix}$$

- State C4+D2 (1, 1):

$$H_{1,0} = \begin{pmatrix} -\frac{1}{4}J + K & -w \\ -w & 2K \end{pmatrix}$$

- State D4 (2, 1/2):

$$H_{2,1/2} = 2K$$

Whether the ground state is a singlet or doublet depends on the relative energies of the lowest energy levels in subspaces  $(-1, 0)$ ,  $(1, 0)$ , and  $(0, 1/2)$ . If the lowest energy level in the subspaces  $(-1, 0)$  and  $(1, 0)$  is lower than the lowest energy level in the subspace  $(0, 1/2)$ , then we have a singlet ( $T\chi$  will approach zero); otherwise, we have a doublet and  $T\chi$  approaches  $1/4$ .

Let us first consider the case  $K_0 \neq 0$ . We perform a second-order perturbation calculation of the energy of the eigenstate with the eigenvalue near  $\frac{3}{4}J + K$ :

- For the subspace  $(-1, 0)$ , we have

$$E_0 \approx \frac{3}{4}J + K + \frac{w^2}{\frac{3}{4}J + K}$$

- For the subspace  $(1, 0)$ , we have

$$E_0 \approx \frac{3}{4}J + K + \frac{w^2}{\frac{3}{4}J - K}$$

- For the subspace  $(0, 1/2)$ , we have

$$E_0 \approx \frac{3}{4}J + K + \frac{1}{2} \frac{w^2}{\frac{3}{4}J + K} + \frac{1}{2} \frac{w^2}{\frac{3}{4}J - K}$$

It is clear that the ground state is always a singlet: when  $K > 0$ , the ground state is in the subspace  $(-1, 0)$ , whereas for  $K < 0$ , the ground state is in the subspace  $(1, 0)$ . The energy level of the first excited state (in subspace  $(0, 1/2)$ ) relative to the ground state is (assuming  $K_0 > 0$ )

$$E_1 \approx \frac{1}{2} \frac{w^2}{\frac{3}{4}J - K} - \frac{1}{2} \frac{w^2}{\frac{3}{4}J + K},$$

which is proportional to  $\Delta$ . The energy level of the second excited state (in subspace  $(Q = 1, S = 0)$ ) is  $E_2 \approx 2E_1$  (this result was also found in our numerical results for the energy levels).

How about  $K_0 = 0$ ? The issue cannot be resolved at the level of second-order perturbation theory. A fourth-order perturbation calculation for the lowest energy in the subspace  $(0, 1/2)$  yields

$$E_0 \approx \frac{3}{4}J + \frac{4}{3} \frac{w^2}{J} + \frac{80}{27} J \left(\frac{w}{J}\right)^4.$$

For the subspaces  $(-1, 0)$  and  $(1, 0)$ , the lowest energy is given by

$$E_0 = \frac{3}{4}J - \sqrt{\left(\frac{3}{4}J\right)^2 + w^2} \approx \frac{3}{4}J + \frac{4}{3} \frac{w^2}{J} - \frac{1}{2} J \left(\frac{w}{J}\right)^4.$$

It is clear that the ground state is in the subspace  $(0, 1/2)$ , which is a doublet. This agrees with our numerical results. The energy gap of the first excited state is proportional to  $w^4$  or  $\Delta^2$ .

## B. Response Function

Let us consider the calculation of  $T \langle\langle S_z; S_z \rangle\rangle$  in the ground state when  $\Delta \ll T_K$ . By definition

$$\langle\langle S_z; S_z \rangle\rangle = \int_0^\beta \langle S_z(\tau) S_z \rangle d\tau.$$

Close to zero temperature, we can write

$$\langle\langle S_z; S_z \rangle\rangle = \sum_{|I\rangle} \frac{|\langle G|S_z|I\rangle|^2 (1 - \exp(-\beta(E_I - E_G)))}{E_I - E_G},$$

where  $|I\rangle$  represents many-body states of the system and  $|G\rangle$  denotes the ground state. For temperatures much smaller than the energy gap between the first excited state and the ground state, we have (separating out the contribution of the ground state from the summation)

$$\langle\langle S_z; S_z \rangle\rangle = \beta |\langle G|S_z|G\rangle|^2 + \sum_{|I\rangle \neq |G\rangle} \frac{|\langle G|S_z|I\rangle|^2}{E_I - E_G}.$$

Since the second term in the above expression is finite, we obtain in the limit as  $T \rightarrow 0$ ,

$$T \langle\langle S_z; S_z \rangle\rangle = |\langle G|S_z|G\rangle|^2.$$

For the case  $K_0 \neq 0$ , it is easy to verify that  $T \langle\langle S_z; S_z \rangle\rangle$  is zero.

For the case that  $K_0 = 0$ , we find that

$$\langle G|S_z|G\rangle = \pm \frac{4w^2}{3J^2}.$$

Thus  $T \langle\langle S_z; S_z \rangle\rangle$  in this case is proportional to  $w^4$  or  $\Delta^2$  in agreement with the numerical results.

## C. Anderson Model

We now discuss the Anderson Model briefly since the results are similar to those of the Kondo problem discussed above. We consider the limit that  $U$  is very large and  $\Gamma$  is very small. The effective Hamiltonian is of the form

$$H_{eff} = \epsilon_d d_\mu^\dagger d_\mu + V(d_\mu^\dagger f_{0\mu} + h.c.) + \Delta(a_\mu^\dagger a_\mu - b_\mu^\dagger b_\mu).$$

Here  $\epsilon_d$  is the effective impurity level at the energy scale  $\Delta$  and  $V$  is the effective coupling to the conduction electron states. The impurity level cannot be doubly occupied:  $n_d \leq 1$ . For the case that  $-\epsilon_d > \Delta$ , then the local moment regime will be reached, and the effective Hamiltonian can be converted to the Kondo Hamiltonian; this has been discussed above. Here we focus on the case that  $-\epsilon_d \ll \Delta$ .

Consider the case when  $V$  is very small; to leading order, the ground state depends on the sign of  $\epsilon_d$ . If  $\epsilon_d > 0$ , then the ground state corresponds to two electrons occupying the conduction electron level at  $-\Delta$ , and it is a singlet (this situation arises, for example, when the initial  $\epsilon_d$  is greater than zero; this has been checked by the nonperturbative RG calculation). If  $\epsilon_d < 0$ , then the ground state corresponds to two electrons occupying the conduction electron level at  $-\Delta$  and one electron occupying the impurity level. So the ground state is a doublet.

From the above analysis, it is clear that the reason for the ground state being a doublet for the case  $-\epsilon_d > \Delta$  (when the local moment regime is reached) and  $-\epsilon_d \ll \Delta$  (when only the mixed-valent regime is reached) are different. In the first case, the local moment regime is reached, and as the temperature is lowered, the moment begins to be quenched due to large effective  $|J|$ , but as the temperature is further lowered, one can see the small splitting of the singlet state to the doublet state due to the finite gap energy. In the second case, the local moment is not formed at the energy scale  $\Delta$ . But as the temperature is lowered to the energy scale of  $-\epsilon_d$ , charge fluctuations are suppressed and they eventually cease to exist, and the system becomes a doublet.



## V. CONCLUSIONS

We have performed a Wilson Renormalization group calculation of the Kondo and Anderson models with a gap in the conduction electron density of states. The impurity susceptibility, correlation functions, and a zero-frequency response function have been calculated as functions of temperatures in various regimes. Our calculations confirm earlier results on the qualitative differences in the low-temperature behaviors between the cases with and without particle-hole symmetry when the gap is much smaller than the Kondo temperature. We have shown that the numerical results at low temperatures can be understood in terms of simple low temperature effective Hamiltonians.

*Acknowledgments* C.J would like to thank the Ohio Supercomputer Center for granting computer time on the Cray.

- 
- <sup>1</sup> K. G. Wilson, *Rev. Mod. Phys.* **47**, 773 (1975).  
<sup>2</sup> P. Nozières, *J. Low Temp. Phys.* **17**, 31 (1974).  
<sup>3</sup> H. R. Krishna-murthy, J. W. Wilkins, and K. G. Wilson, *Phys. Rev. B* **21**, 1003 and 1044 (1980).  
<sup>4</sup> L. Cruz, P. Phillips, and A. H. Castro Neto, *Europhys. Lett.*, **29**, 389 (1995).  
<sup>5</sup> H. Takayama, Y. R. Lin-Liu, and K. Maki, *Phys. Rev. B* **21**, 2388 (1980).  
<sup>6</sup> K. Chen and C. Jayaprakash, *Phys. Rev. B* **52**, 14436. (1995).  
<sup>7</sup> Kan Chen, C. Jayaprakash, and H.R. Krishnamurthy, *Phys. Rev. B* **45**, 5368-5386 (1992).  
<sup>8</sup> Kan Chen and C. Jayaprakash, *J. Phys: Condens. Matter* **7**, L491 (1995).  
<sup>9</sup> T. Saso, *J. Phys. Soc. Jpn.* **61**, 3439 (1992)  
<sup>10</sup> T. Saso and J. Ogura, *Physica B* **186-188**, 372 (1993)  
<sup>11</sup> J. Ogura and T. Saso, *J. Phys. Soc. Jpn.* **62**, 4364 (1993)  
<sup>12</sup> K. Takegahara, Y. Shimizu, and O. Sakai, *J. Phys. Soc. Jpn.* **61**, 3443 (1992)  
<sup>13</sup> K. Takegahara, Y. Shimizu, N. Goto, and O. Sakai, *Physica B* **186-188**, 381 (1993)  
<sup>14</sup> C. C. Yu and M. Guerrero, *Phys. Rev. B* **54**, 8556 (1996)  
<sup>15</sup> K. Ingersent, *Phys. Rev. B* **54**, 11936 (1996)

FIG. 1.  $T\chi_{imp}$  plotted as a function of  $T$  for the Kondo problem. The gap energy is  $\Delta = 1.22 \times 10^{-4}$ . (a) The potential scattering is absent ( $K = 0.0$ ). The values of the coupling  $J$  used are  $-0.1, -0.2, -0.3, -0.4$ , and  $-1.0$ . Note that as  $T \rightarrow 0$ ,  $T\chi$  approaches  $1/4$ . (b) Particle-hole symmetry breaking is present ( $K = 0.1$ ). Note that for  $J = -0.4$ ,  $T\chi$  goes to zero, while for  $J = -0.2$ , it approaches  $1/4$ .

FIG. 2.  $T\chi_{imp}$  plotted as a function of  $T$  for the Anderson model. (a) Symmetric Anderson model with  $U = 0.1, \epsilon_d = -0.05$ , and  $\Gamma = 0.006$ . Note that as  $T \rightarrow 0$ ,  $T\chi$  approaches  $1/4$ . (b) Asymmetric Anderson model with  $U = 0.1, \epsilon_d = -0.001$ , and  $\Gamma = 0.00015$ . Note that as  $T \rightarrow 0$ ,  $T\chi$  approaches  $1/4$  if  $\Delta \gg T_K$  and 0 if  $\Delta \ll T_K$ . The values for the gap energy  $\Delta$  used in the calculations are shown in the legends of the figures.

FIG. 3. The zero-frequency response function  $T \ll S_z; S_z \gg$  plotted as a function of  $T$  for the asymmetric Anderson model with  $U = 0.1, \epsilon_d = -0.001$ , and  $\Gamma = 0.00015$ . Note the qualitative differences between  $T \ll S_z; S_z \gg$  and  $T\chi$  at low temperatures.

FIG. 4. The local correlation functions: (a)  $\langle n_d \rangle$  and (b)  $\langle \vec{S} \cdot \vec{\sigma}(0) \rangle$ , plotted as a function of  $T$  for the asymmetric Anderson model with  $U = 0.1, \epsilon_d = -0.001$ , and  $\Gamma = 0.00015$ . Note that when  $\Delta \ll T_K$ , the correlation functions approach constant values independent of  $\Delta$  as  $T \rightarrow 0$ .

FIG. 5. The impurity susceptibility (Fig. 5(a)),  $\langle n_d \rangle$  (Fig. 5(b)), and  $T \ll S_z; S_z \gg$  (Fig. 5(c)), plotted as a function of  $T$  for the asymmetric Anderson model with  $U = 0.1, \epsilon_d = -0.025$ , and  $\Gamma = 0.01$ .

TABLE I. The values of  $T \langle\langle S_z; S_z \rangle\rangle$  at zero temperature for a range of values of the band gap. The numbers enclosed in the parentheses are the total charge  $Q$  and spin  $S$  of the ground state.

| $\Delta$              | $J_0 = -0.2, K = 0.0$ | $J_0 = -0.2, K = 0.0$          |
|-----------------------|-----------------------|--------------------------------|
| $1.88 \times 10^{-6}$ | 0.0398 (0, 1/2)       | 0.0490 (0, 1/2)                |
| $6.27 \times 10^{-7}$ | 0.00797 (0, 1/2)      | 0.0110 (0, 1/2)                |
| $2.09 \times 10^{-7}$ | 0.00101 (0, 1/2)      | $< 1.2 \times 10^{-5}$ (-1, 0) |
| $6.96 \times 10^{-8}$ | 0.000115 (0, 1/2)     | $< 4.0 \times 10^{-6}$ (-1, 0) |

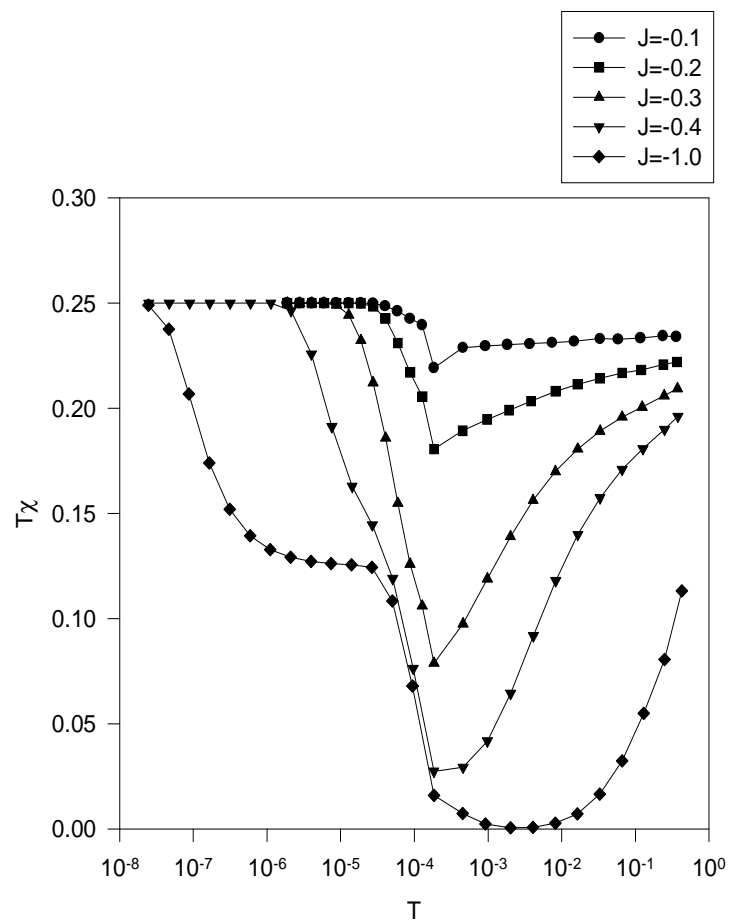


Fig. 1(a)

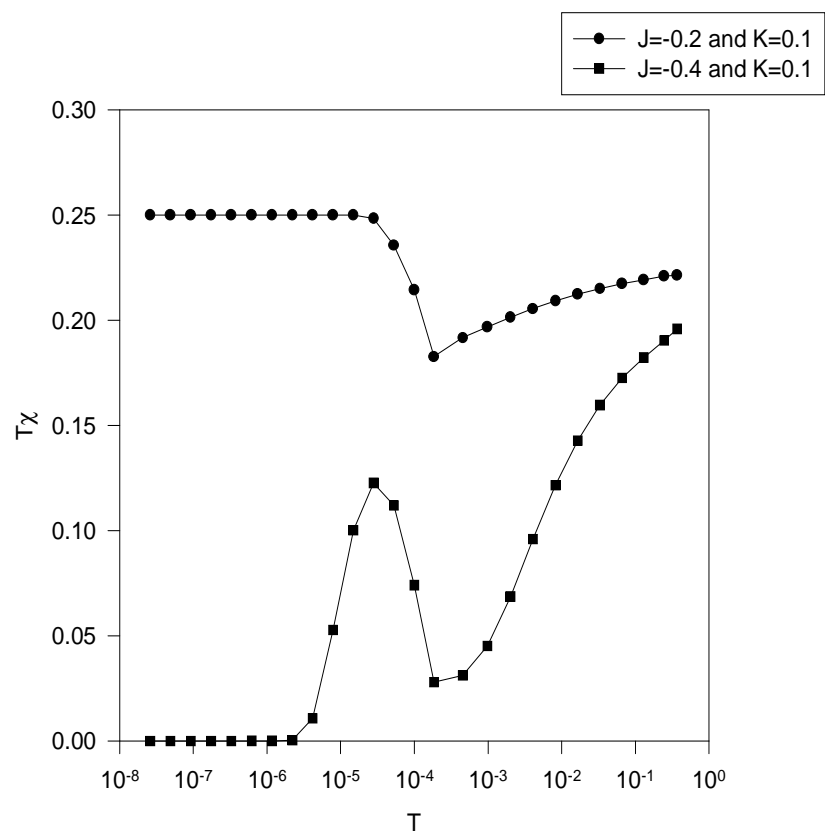


Fig. 1(b)

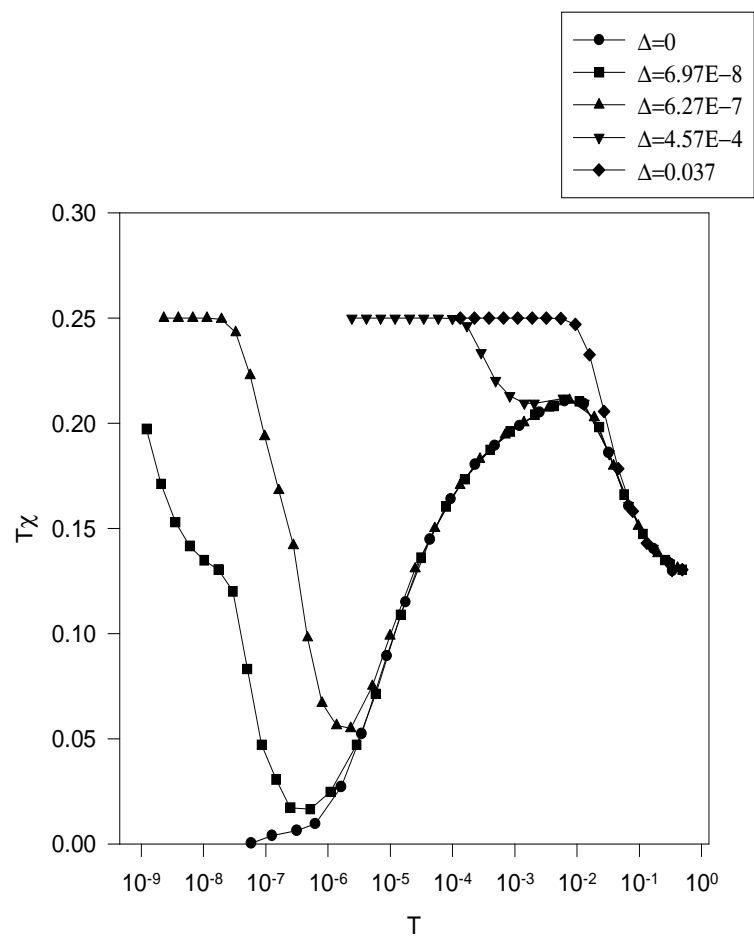


Fig. 2(a)

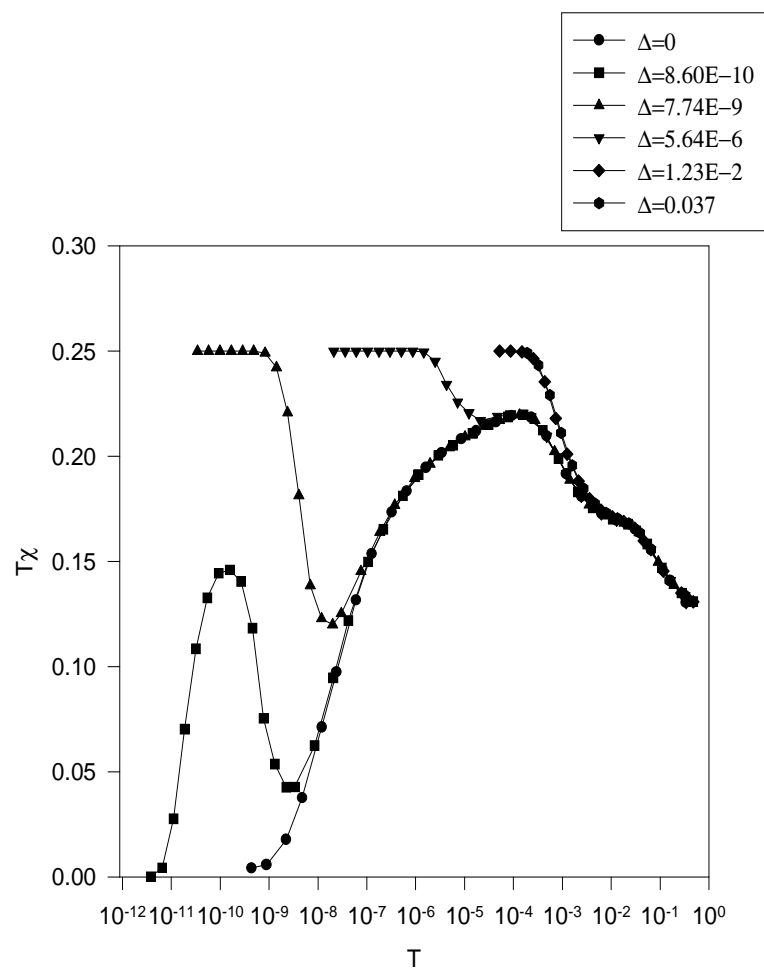


Fig. 2(b)

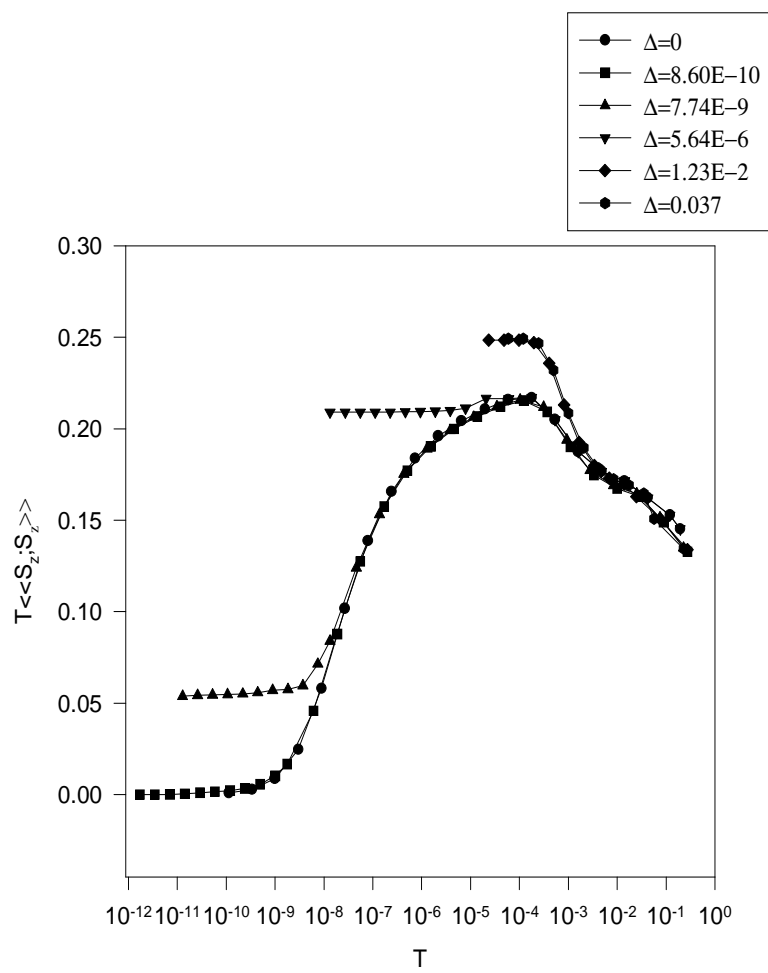


Fig. 3

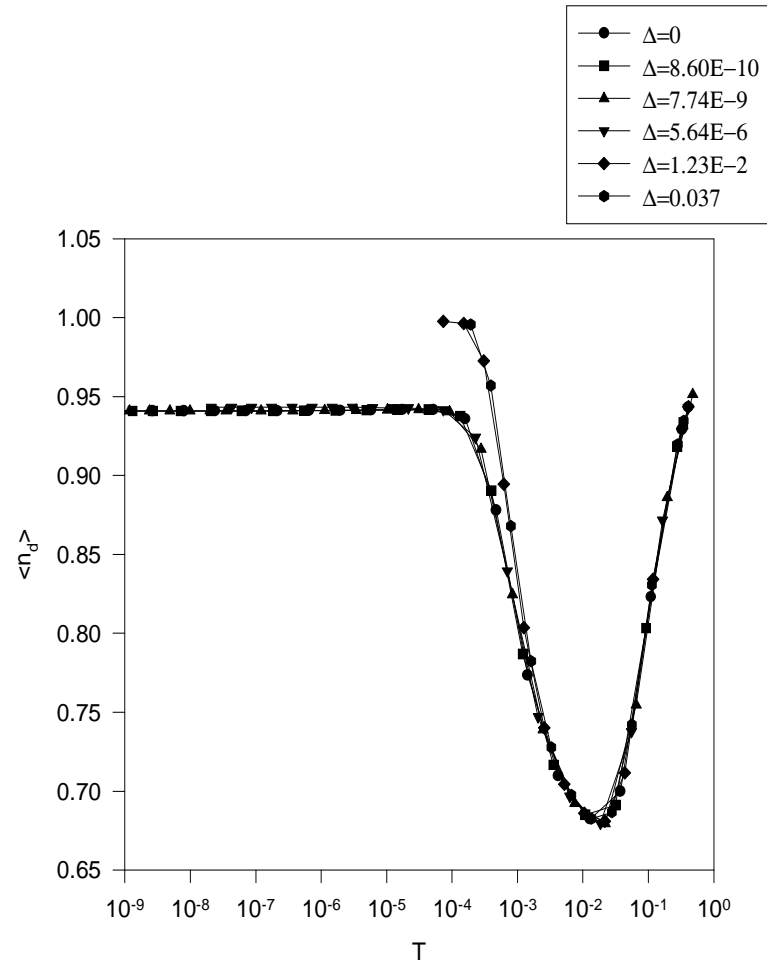


Fig. 4(a)



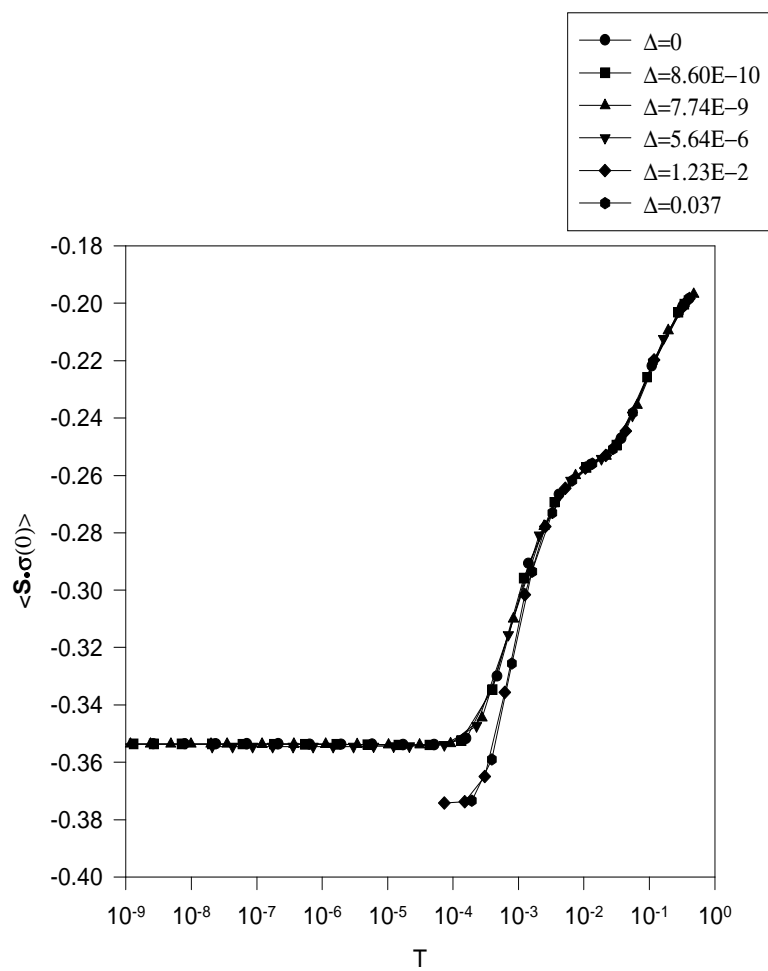


Fig. 4(b)

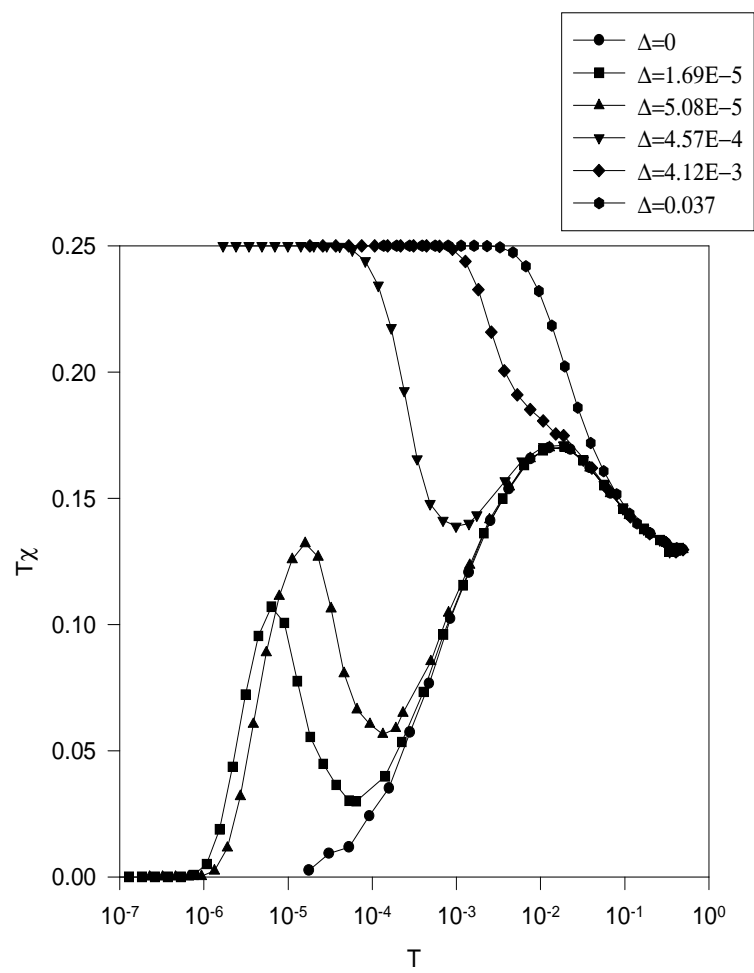


Fig. 5(a)

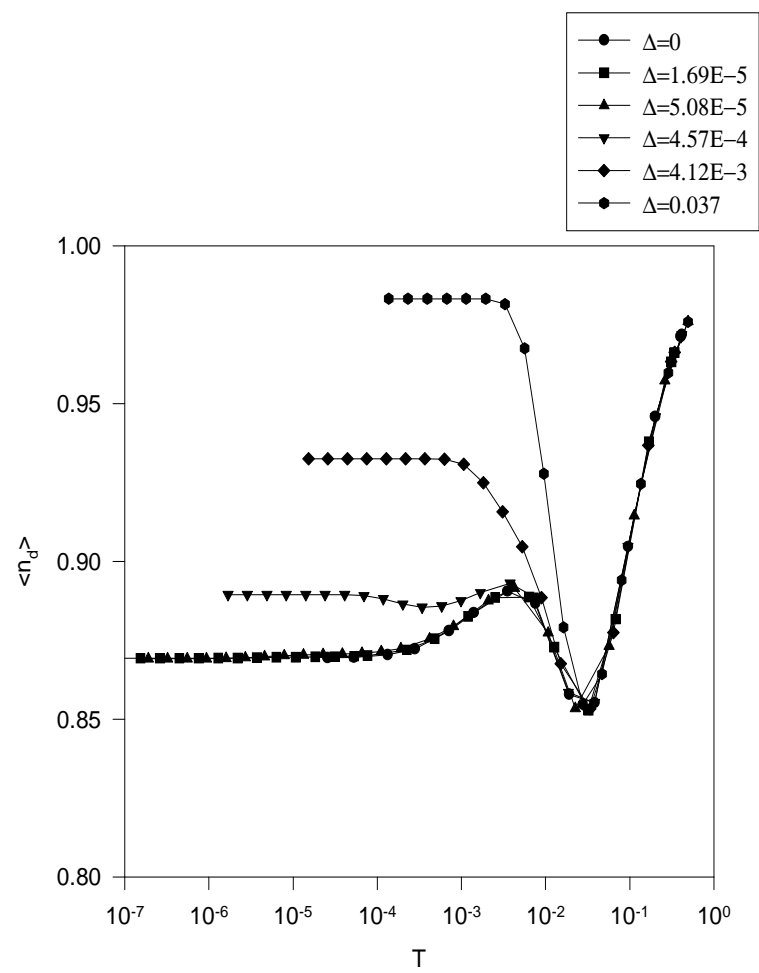


Fig. 5(b)

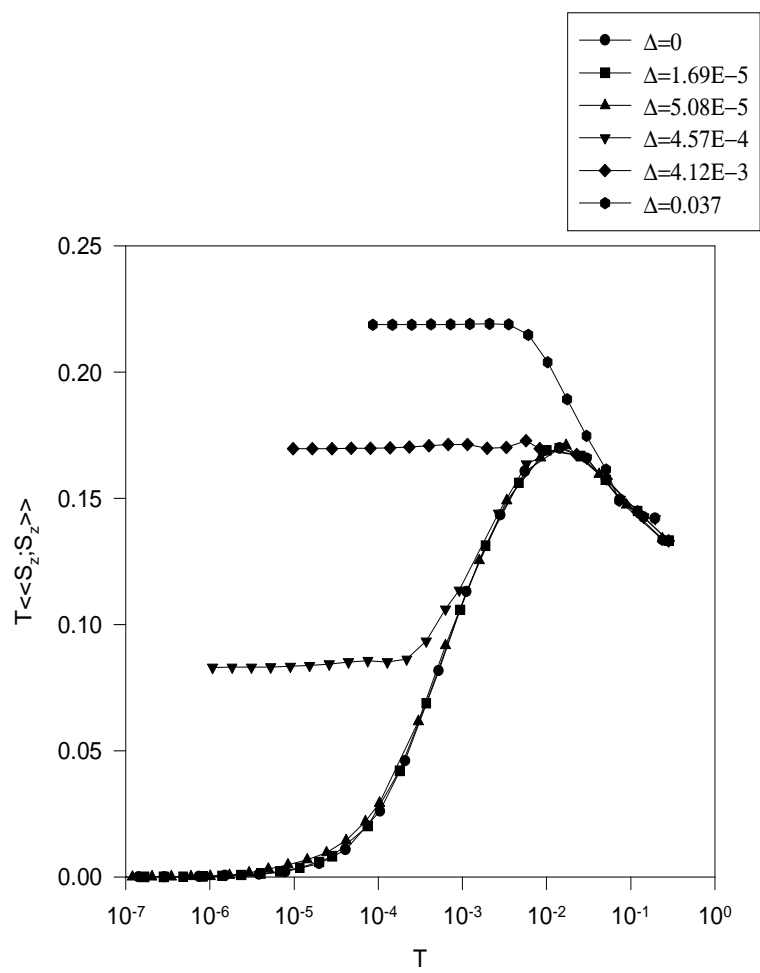


Fig. 5(c)